TECHNICAL ARTICLE

50 kGy of gamma irradiation does not affect the leachability of mineral soils and sediments

Damian B. Gore,[1,a] and Ian Snape[2]
[1]*Department of Environment and Geography, Macquarie University, NSW 2109, Australia*
[2]*Australian Antarctic Division, 203 Channel Highway, Tasmania 7050, Australia*

(Received 3 September 2014; accepted 19 September 2014)

Sterilization of soils and sediments can release them from quarantine restrictions. Gamma irradiation is effective at sterilization but can damage materials and in so doing affect their suitability for environmental research. Duplicate samples of a wide range of mineral soils and sediments were subject to an acetic acid extraction before and after 50 kGy gamma irradiation. This amount of gamma irradiation did not affect the leachability of a range of analytes from the soils and sediments. © *2014 International Centre for Diffraction Data*. [doi:10.1017/S0885715614000918]

Key words: environment, TCLP, mineralogy, crystallinity

I. INTRODUCTION

Gamma irradiation is a common method of killing insects and microorganisms in foods, preventing premature spoilage, and extending the shelf life of many products. Sterilization occurs in a range of ways, including radiation damage directly to organisms, or by free radicals generated particularly by radiolysis of water. Sterilization by gamma irradiation is used commercially for food, industrial applications with organic and inorganic materials, and for quarantine purposes (particularly for soil materials, e.g. McLaren *et al.*, 1962; Popenoe and Eno, 1962; Eno and Popenoe, 1964; Brown, 1981). Gamma irradiation affects solid inorganic materials either by lattice reorganization, atomic dislocation (Kinchin and Pease, 1955), charge separation, or the hydrolysis of water into oxidizing and reducing species which may change the oxidation–reduction potential of soil water, however, the extent to which this affects the leachability of inorganic analytes in soils sampled for environmental research is little known. Some of our research, particularly regarding contaminant leachability, involves manipulative experiments using Antarctic soils and sediments (e.g. Stark *et al.*, 2008) which must be carried out in quarantine-approved premises. The ability to release those soils and sediments from quarantine restrictions expedites multi-institutional research in non-approved premises. Release from Australian quarantine restrictions can occur via treatment with heat, chemical sterilants (methyl bromide or ethylene oxide), or irradiation (DAFF, 2013). Heat and chemicals would render the soils and sediments unfit for some research, and irradiation remains the preferred treatment. The Australian Quarantine and Inspection Service require 50 kGy of gamma radiation to release materials from quarantine restrictions. That radiation damage can occur to materials is undisputed, and what is unclear is the impact of the damage caused by 50 kGy of gamma irradiation on the potential for enhanced leachability of a range of inorganic analytes.

Irradiation of soil is an effective way to ensure sterilization and this is the basis for its use to ensure compliance with national quarantine and import/export requirements. Fungi are understood to be the most sensitive part of the soil microflora and fauna, with fungal viability destroyed with 0.8 Mrad (8 kGy) of gamma radiation (Jackson *et al.*, 1967), and with fauna including bacteria and actinomycetes persisting to 2.2 Mrad (22 kGy) and being destroyed with 4 Mrad (40 kGy) (Jackson *et al.*, 1967; Brown, 1981).

Very few studies so far have examined the effects of gamma irradiation on the crystallinity of natural minerals. Aygun *et al.* (2012) report pre- and post-irradiation X-ray diffractometry from trommel sieve waste. Their Figure 5 shows an increase in crystallinity after irradiation, with their Table 2 reporting a much greater intensity for the most intense peak in the waste. X-ray fluorescence spectrometry of the waste (their Table 1) indicates that a composition largely of Mg, Si, and Ca with subdominant B and a range of other minor and trace elements. The mineral with the 100% reflectance peak at 30.2°2θ is unidentified, and despite the dominance of Si and Ca in the bulk elemental analysis, the peaks do not belong to aragonite, calcite, or quartz. It is unexplained why this mineral might become more crystalline with irradiation, or whether this was an artifact of subsampling a heterogeneous bulk material. As a consequence, it is not clear whether this result is reproducible.

Silicate glasses and minerals may also be prone to radiation damage. Some glasses and minerals can change color as radiation-induced electron hole centers form (Dias *et al.*, 2009). For example, the monoclinic mineral euclase [$BeAlSiO_4(OH)$] exhibited damage at doses of 10–500 kGy, with damage also recorded for other minerals, including the trigonal mineral quartz and amorphous silica (SiO_2, Pantelides *et al.*, 2008), the complex and highly compositionally variable trigonal borosilicate-mineral tourmaline [$XY_3Z_6(T_6O_{18})(BO_3)_3X_3Z$] (Krambrock *et al.*, 2004), and the orthorhombic mineral topaz [$Al_2SiO_4(F,OH)_2$, da Silva *et al.*, 2005]. Further evidence of mineral structural-change by extreme (1000 and 6000 kGy) irradiation is found in Cr-bearing spinel created artificially by heating hydrotalcite

[a]Author to whom correspondence should be addressed. Electronic mail: damian.gore@mq.edu.au

TABLE I. Summary of samples for TCLP extraction. Samples are from the state of NSW in Eastern Australia ($n = 16$) or Antarctica ($n = 9$). (_R) indicates a duplicate sample for QA/QC.

Code	Provenance	Mineralogy
	Sediment 1 – Carbonate-rich beach sands	
Curl Curl	Beach sand, Curl Curl Beach, NSW	Aragonite, Calcite, Quartz
Narrabeen	Beach sand, Narrabeen Beach, NSW	Aragonite, Calcite, Quartz
	Soil 1 – Quartz-poor basaltic substrates	
WA_2	Soil on basalt/qtz sandstone, Mt Wilson, NSW	Anatase, Chromite, Hematite, Kaolinite, Quartz
WA_3	Soil on basalt/qtz sandstone, Mt Wilson, NSW	Albite, Kaolinite, Microcline, Quartz
WF/I	Soil on basalt/qtz sandstone, Mt Wilson, NSW	Anatase, Birnessite, Hematite, Quartz
WF/IIB20-28	Soil on basalt/qtz sandstone, Mt Wilson, NSW	Anatase, Hematite, Kaolinite, Magnetite, Quartz
WF/IIB20-28_R	Soil on basalt/qtz sandstone, Mt Wilson, NSW	Anatase, Hematite, Kaolinite, Magnetite, Quartz
	Soil 2 – Quartz-rich sandstone substrates	
MF2_3	Soil on Hawkesbury sandstone, Newnes, NSW	Anatase, Dickite, Kaolinite, Quartz
NewnesQuarry	Soil on Hawkesbury sandstone, Newnes, NSW	Anatase, Dickite, Kaolinite, Quartz
Polpah_4a60	Siliceous sand, White Cliffs, NSW	Albite, Kaolinite, Montmorillonite, Quartz
Polpah_5c60	Siliceous sand, White Cliffs, NSW	Albite, Kaolinite, Muscovite, Orthoclase, Quartz
	Sediment 2 – Antarctic glacial sediments	
B10_G	Prince Charles Mountains, East Antarctica	Albite, Clinopyroxene, Kaolinite, Microcline, Quartz
B15_G	Prince Charles Mountains, East Antarctica	Kaolinite, Microcline, Muscovite, Quartz, Zircon
G8_G	Prince Charles Mountains, East Antarctica	Albite, Cristobalite, Quartz, Microcline, Phlogopite
G60_G	Prince Charles Mountains, East Antarctica	Albite, Quartz, Muscovite, Orthoclase
VH04SS134	Vestfold Hills, East Antarctica	Clinoenstatite, Magnesiohornblende, Plagioclase, Quartz
VH04SS138	Vestfold Hills, East Antarctica	Albite, Magnesiohornblende, Microcline, Quartz
VH04SS139	Vestfold Hills, East Antarctica	Albite, Magnesiohornblende, Microcline, Muscovite, Quartz
VH04SS140	Vestfold Hills, East Antarctica	Albite, Magnesiohornblende, Microcline, Muscovite, Quartz
VH04SS140_R	Vestfold Hills, East Antarctica	Albite, Magnesiohornblende, Microcline, Muscovite, Quartz
	Mineralized base metal ores	
EyreSt	Broken Hill Pb–Zn–Ag ore, NSW	Muscovite, Quartz, Zircon
EyreSt_R	Broken Hill Pb–Zn–Ag ore, NSW	Muscovite, Quartz, Zircon
VS2/4/Salt	Broken Hill Pb–Zn–Ag ore, NSW	Illite, Jordanite, Litharge, Microcline, Quartz, Zircon
VS2/5/Blue	Broken Hill Pb–Zn–Ag ore, NSW	Birnessite, Calcite, Muscovite, Quartz
Woodsreef	Chromite ore, Woodsreef, NSW	Muscovite, Quartz, Zircon

$[Mg_6Al_2(OH)_{16}[CO_3].4H_2O]$ to 1200 °C. Leaching using a NaCl solution revealed that irradiated spinel retained Cr more strongly than non-irradiated spinel, and that a larger dose of gamma radiation led to lower desorption of Cr, either because of the development of a preferential crystallite-orientation or relocation of Cr ions in the crystal structure (Martinez-Gallegos and Bulbulian, 2004).

Clay minerals have differing susceptibilities to radiation, with the onset of damage ranging over several orders of magnitude of irradiation from 100 kGy for brucite $[Mg(OH)_2]$ and kaolinite $[Al_2(Si_2O_5)(OH)_4]$, 1000 kGy for montmorillonite $[(Na,Ca)_{0.33}(Al, Mg)_2(Si_4O_{10})(OH)_2.nH_2O]$ and palygorskite $[(Mg,Al)_5(Si,Al)_8O_{20}(OH)_2.8H_2O)]$, to 30 000 kGy for gibbsite $[Al(OH)_3]$ (Pushkareva *et al.*, 2002). Of the minerals tested, kaolinite had the greatest number of radiation-induced defects and was the most susceptible clay mineral to radiation damage. A test of leachability with 0 vs 30 000 kGy of gamma radiation generally showed decreased release of Si (44–138%), and increased the release of Al (105–144%), and increases in specific surface area (105–131%). However, changes in the surface area, cation exchange capacity, and main-layer charge were found to be weak for clays with gamma irradiation up to 1100 kGy (Plötze *et al.*, 2003). These results are consistent with Negron *et al.* (2002) who found that 2000 kGy of gamma irradiation had no observable effect on montmorillonite, unlike Pyrex glass that turns black with the same exposure. One of the reasons montmorillonite may be resistant to radiation-induced damage is that structural Fe or adsorbed organics in the clay can act as a sink for some of the oxidants produced as a consequence of hydrolysis of water (Holmboe *et al.*, 2012). Importantly, clay can also act to enhance the production of oxidizers such as H_2O_2 (Fattahi *et al.*, 1992), increasing the potential significance of understanding these reactions on soil–metal interactions.

The effects of gamma irradiation on the crystallinity of kaolinite are equivocal, with increasing crystallinity with 2 kGy of irradiation, and then weakly decreasing crystallinity with up to 100 kGy irradiation, and no change in crystallinity with kaolinite that was poorly crystalline at the commencement of the experiment (Corbett *et al.*, 1963). The Hinckley Index for the crystallinity of kaolinite revealed equivocal results for 100 kGy exposure (Plötze *et al.*, 2003). Gamma irradiation can increase the stability of colloidal dispersions in a dilute NaCl solution, possibly owing to changes in the colloids' surface-potential because of reactions with radiolysis products (Holmboe *et al.*, 2009).

It remains unclear whether or not gamma irradiation changes soils and sediments that might subsequently be used for mineralogical or selective extraction-tests for environmental assessment. Such tests include the Synthetic Precipitation Leaching Procedure (SPLP; USEPA Method, 1312) or weak acid [e.g. Toxicity Characteristic Leaching Procedure (TCLP); USEPA Method, 1311] extractions. There are clear mechanisms that might change crystallinity, degrade compounds (particularly organics), and the possibility of creating oxidizing and reducing compounds (Holmboe

https://doi.org/10.1017/S0885715614000918 Published online by Cambridge University Press

TABLE II. TCLP leachate data.

Sample	Soil	Fluid	Leachate	Mg	Al	S	K	Ca	Cr	Mn	Fe	Ni	Cu	Zn	Zr	Cd	Pb
Units	pH	pH	pH	mg l^{-1}	mg l^{-1}	mg l^{-1}	mg l^{-1}	mg l^{-1}	mg l^{-1}	mg l^{-1}	mg l^{-1}	mg l^{-1}	mg l^{-1}	mg l^{-1}	mg l^{-1}	mg l^{-1}	mg l^{-1}
PQL	<0.1	<0.1	<0.1	<0.03	<0.1	<0.5	<0.03	<0.03	<0.01	<0.01	<0.02	<0.02	<0.01	<0.02	<0.02	<0.01	<0.03
Carbonate-rich beach sands																	
CurlCurl_A	6.6	1.6	5.0	2.5	<0.1	1.1	3.6	40	<0.01	0.03	0.09	<0.02	0.03	0.4	<0.02	<0.01	<0.03
CurlCurl_B	6.9	1.6	5.0	2.6	<0.1	1.0	<0.03	38	<0.01	0.03	0.09	<0.02	0.03	0.5	<0.02	<0.01	<0.03
Narrabeen_A	8.2	1.6	6.4	37	<0.1	5.7	<0.03	570	<0.01	0.4	0.06	<0.02	0.02	0.6	<0.02	<0.01	<0.03
Narrabeen_B	8.1	1.7	6.3	39	<0.1	5.8	<0.03	590	<0.01	0.4	0.05	<0.02	0.02	0.4	<0.02	<0.01	<0.03
Quartz-poor basalt substrates																	
WA_2_A	8.3	1.6	5.0	2.1	1.6	5.1	2.5	4.4	<0.01	0.2	0.02	<0.02	0.03	0.5	<0.02	<0.01	0.2
WA_2_B	8.0	1.7	5.0	2.4	1.7	5.3	6.4	4.1	<0.01	0.5	0.04	<0.02	0.06	1.2	<0.02	<0.01	0.2
WA_3_A	8.6	1.8	5.0	18	<0.1	1.2	8.0	58	<0.01	0.5	0.02	<0.02	0.04	0.6	<0.02	<0.01	0.2
WA_3_A_R	[NT]	[NT]	[NT]	17	<0.1	1.2	8.0	57	<0.01	0.5	0.02	<0.02	0.04	0.6	<0.02	<0.01	0.2
WA_3_B	8.6	1.9	5.0	18	0.1	1.1	8.0	60	<0.01	0.6	0.04	<0.02	0.03	0.4	<0.02	<0.01	0.1
WF/I_A	8.0	1.6	4.9	5.8	2.1	2.4	7.4	10	<0.01	0.9	0.1	<0.02	0.03	0.6	<0.02	<0.01	0.08
WF/I_B	6.3	1.6	5.0	5.6	2.6	2.4	4.7	9.2	<0.01	1.1	0.2	<0.02	0.04	0.6	<0.02	<0.01	0.09
WF/IIB_20-28_A	6.3	1.6	4.9	2.8	1.9	3.5	1.3	3.2	<0.01	3.4	0.04	<0.02	0.02	0.5	<0.02	<0.01	0.05
WF/IIB_20-28_B	6.1	1.7	5.0	3.4	2.2	4.1	1.6	3.7	<0.01	0.8	0.05	<0.02	0.02	0.5	<0.02	<0.01	0.05
WF/IIB_20-28R_A	6.2	1.6	5.0	3.1	1.9	3.8	1.5	3.6	<0.01	0.4	0.03	<0.02	0.03	0.5	<0.02	<0.01	0.04
WF/IIB_20-28R_B	6.0	1.6	5.0	3.2	2.1	4.0	1.6	3.6	<0.01	0.7	0.05	<0.02	0.02	0.5	<0.02	<0.01	0.03
Quartz-rich sandstone substrates																	
MF2_3_A	8.0	1.6	5.0	1.0	0.9	0.8	<0.03	2.1	<0.01	0.04	0.04	<0.02	0.02	0.5	<0.02	<0.01	0.07
MF2_3_B	5.6	1.6	4.9	1.1	0.9	0.8	<0.03	2.3	<0.01	0.05	0.08	<0.02	0.03	1.1	<0.02	<0.01	0.09
NewnesQuarry_A	7.7	1.6	5.0	0.8	0.5	<0.5	<0.03	3.5	<0.01	0.03	<0.02	<0.02	0.03	0.5	<0.02	<0.01	0.07
NewnesQuarry_B	6.2	1.7	4.9	0.9	0.5	0.6	<0.03	2.5	<0.01	0.03	<0.02	<0.02	0.04	0.8	<0.02	<0.01	0.09
Polpah_4a60_A	7.5	1.6	4.9	14	<0.1	<0.5	8.5	45	<0.01	0.1	<0.02	<0.02	0.03	0.5	<0.02	<0.01	0.06
Polpah_4a60_B	7.8	1.6	4.9	14	<0.1	0.7	8.1	44	<0.01	0.9	<0.02	<0.02	0.04	0.5	<0.02	<0.01	0.03
Polpah_5c60_A	8.4	1.7	4.9	6.5	<0.1	<0.5	12	25	<0.01	0.1	<0.02	<0.02	0.03	0.5	<0.02	<0.01	0.04
Quartz-rich sandstone substrates (continued)																	
Polpah_5c60_A_R	[NT]	[NT]	[NT]	6.4	<0.1	<0.5	12	25	<0.01	0.1	<0.02	<0.02	0.03	0.5	<0.02	<0.01	0.03
Polpah_5c60_B	8.5	1.6	5.0	6.4	<0.1	<0.5	12	24	<0.01	1.1	0.02	<0.02	0.02	0.4	<0.02	<0.01	<0.03
Antarctic glacial sediments																	
B10_G_A	7.6	1.6	5.0	18	0.1	0.8	6.1	62	<0.01	0.6	0.05	<0.02	0.03	0.4	<0.02	<0.01	<0.03
B10_G_A_R	[NT]	[NT]	[NT]	19	0.1	1.0	5.9	62	<0.01	0.6	0.04	<0.02	0.03	0.4	<0.02	<0.01	<0.03
B10_G_B	8.9	1.6	5.1	19	0.1	1.1	6.1	64	<0.01	0.7	0.06	<0.02	0.03	0.4	<0.02	<0.01	<0.03
B15_G_A	7.2	1.7	5.0	3.3	<0.1	1.9	<0.03	5.1	<0.01	0.4	0.03	<0.02	0.02	0.5	<0.02	<0.01	<0.03
B15_G_B	6.4	1.6	5.0	3.1	<0.1	1.9	<0.03	4.8	<0.01	0.5	0.02	<0.02	0.03	0.5	<0.02	<0.01	<0.03
G8_G_A	9.1	1.6	5.0	3.9	<0.1	<0.5	<0.03	8.8	<0.01	0.1	<0.02	<0.02	0.03	0.6	<0.02	<0.01	0.3
G8_G_A_R	[NT]	[NT]	[NT]	4.0	<0.1	<0.5	<0.03	9.1	<0.01	0.1	<0.02	<0.02	0.03	0.7	<0.02	<0.01	0.3
G8_G_B	8.8	1.7	5.0	4.1	<0.1	<0.5	<0.03	8.6	<0.01	0.2	<0.02	<0.02	0.03	0.6	<0.02	<0.01	0.1
G60_G_A	9.0	1.8	4.9	6.3	<0.1	0.6	1.6	7.8	<0.01	0.5	<0.02	<0.02	0.03	0.5	<0.02	<0.01	0.1
G60_G_B	8.7	1.6	4.9	6.1	<0.1	0.5	1.2	7.7	<0.01	0.6	<0.02	<0.02	0.03	0.6	<0.02	<0.01	0.08
VH04SSI34_A	9.4	1.7	5.1	11	0.2	5.8	9.2	100	<0.01	1.4	0.03	0.04	0.3	3.1	<0.02	<0.01	0.07
VH04SSI34_B	9.5	1.6	5.1	11	0.3	6.4	12	110	<0.01	1.6	0.06	0.04	0.4	3.8	<0.02	0.01	0.08
VH04SSI38_A	9.5	1.6	5.0	4.6	0.4	2.0	4.0	36	<0.01	1.0	0.1	0.03	0.3	1.5	<0.02	<0.01	0.1
VH04SS138_B	9.2	1.6	4.9	4.5	0.4	2.0	4.3	35	<0.01	1.0	0.1	0.03	0.2	1.6	<0.02	<0.01	0.1
VH04SSI39_A	9.3	1.6	5.0	4.4	0.1	3.0	4.8	36	<0.01	1.1	0.09	0.03	0.5	3.6	<0.02	0.03	0.9
VH04SSI39_B	9.2	1.6	5.0	4.0	0.1	2.8	5.0	32	<0.01	1.0	0.1	0.03	0.5	3.4	<0.02	0.03	0.7
VH04SSI40_A	8.9	1.6	5.0	4.4	<0.1	3.4	3.5	17	<0.01	0.8	0.09	0.03	0.1	0.9	<0.02	<0.01	0.07
VH04SSI40_A_R	[NT]	[NT]	[NT]	4.5	<0.1	3.4	3.5	18	<0.01	0.8	0.09	0.03	0.1	0.9	<0.02	<0.01	0.06

VH04SSI40_B	8.7	1.6	5.0	4.4	<0.1	3.5	3.4	17	<0.01	0.9	0.1	0.03	0.09	0.9	<0.02	<0.01	0.05
VH04SSI40R_A	8.7	1.6	5.0	3.9	<0.1	2.9	3.4	15	<0.01	0.7	0.1	0.03	0.08	0.9	<0.02	<0.01	0.05
VH04SSI40R_B	7.4	1.7	5.0	4.0	<0.1	3.1	3.4	15	<0.01	0.8	0.1	0.03	0.07	1.0	<0.02	<0.01	0.06
Mineralized samples																		
EyreStreet_A	8.4	1.7	5.5	19	0.1	14	16	350	<0.01	1.5	0.02	<0.02	0.1	27	<0.02	0.2	26
EyreStreet_B	8.6	1.6	5.5	19	0.1	13	11	330	<0.01	1.8	0.02	<0.02	0.09	26	<0.02	0.2	25
EyreStreetR_A	8.7	1.7	5.6	20	0.1	16	13	350	<0.01	1.6	0.04	<0.02	0.1	29	<0.02	0.3	28
EyreStreetR_B	8.8	1.6	5.5	19	0.1	14	11	330	<0.01	1.9	<0.02	<0.02	0.1	28	<0.02	0.3	28
VS2/4/Salt_A	6.8	1.6	5.0	3.4	1.2	21	4.9	32	<0.01	4.4	0.4	0.02	0.4	56	<0.02	0.2	82
VS2/4/Salt_B	6.9	1.6	5.0	3.4	1.3	22	4.7	32	<0.01	4.9	0.6	0.02	0.4	59	<0.02	0.2	83
VS2/5/Blue_A	8.0	1.6	5.0	51	<0.1	130	14	610	<0.01	0.8	<0.02	<0.02	0.03	1.0	<0.02	0.02	0.6
VS2/5/Blue_B	8.3	1.7	6.1	47	<0.1	120	11	580	0.2	1.2	<0.02	<0.02	0.04	0.9	<0.02	0.02	0.4
Woodsreef_A	6.0	1.6	5.0	110	0.9	4.6	6.6	29	0.2	8.3	0.8	1.9	0.04	0.6	0.2	<0.01	0.05
Woodsreef_B	6.2	1.8	5.0	110	1.0	5.0	7.2	31	<0.02	8.8	0.9	2.1	0.04	0.5	0.1	<0.01	0.07

"_A" = untreated, "_B" = irradiated, "_R" = replicate. All Ti < 0.02, As < 0.05, Se < 0.12, Zr < 0.02, Sn < 0.05, Sb < 0.15 mg l^{-1}. PQL = Practical Quantitation Limit, [NT] = not tested.

et al., 2012) as well as free radicals that might damage the reservoirs where elements of concern (such as heavy metals) might reside. If this is the case, then gamma-irradiation-induced change might enhance leachability of elements in environmental tests, potentially leading to inaccurate, and erroneous data. Gamma irradiation at 7670 kGy increases the leachability of Co (Dávila-Rangel *et al.*, 2007), Cd (Dávila-Rangel and Solache-Ríos, 2008), and presumably other metal ions in aluminosilicates, although the effects of sample heating on mineralogy are greater than irradiation, even at the relatively large irradiation doses received in these studies. Similarly, gamma irradiation of Cu metal created radiation-enhanced corrosion at doses of 20 kGy and greater, probably because of enhanced galvanic action between the surface copper oxide layer and the zero-valent metal beneath (Björkbacka *et al.*, 2013).

This research focuses on the assessment of irradiation damage to selected natural soils and sediments. To understand potential impacts of irradiation, the leachability (using the TCLP; USEPA Method, 1311) of 25 soils and sediments were assessed before and after exposure to 50 kGy of gamma radiation, which is the amount required by the Australian Quarantine and Inspection Service for the release of such materials from quarantine control.

II. EXPERIMENTAL

To evaluate the effects of gamma irradiation, a wide range of soils and sediments were selected from semi-arid, temperate, and coastal Australia as well as dry-frigid Antarctica, to represent a broad range of mineralogical provenance and depositional and pedogenic processes (Table I). Soils were formed on mixed basalt/quartz sandstone or quartz sandstone, sediments were from beaches, semi-arid lands, or Antarctica, and there were two types of weathered base-metal ore. The soils formed from basalt had a gradational principal profile form (Northcote, 1979), whereby the clay content became greater and texture became finer down-profile. The quartz sandstone developed a soil with a duplex principal profile form, whereby there was a sharp mineralogical and textural transition between the A and B horizons. The beach sediments were siliceous sands with a substantial biogenic aragonite and calcite component. The floodplain sediments had accumulated from the erosion of intercalated sandstones and siltstones. The glacial sediments had a very complex provenance from high-grade metamorphic and sedimentary terranes. The ore material lay adjacent to the skimp heaps atop a Pb–Zn–Ag deposit, which in places may have received aeolian accessions of ore concentrate.

Bulk dry soil of at least 200 g (Table I) was obtained and sieved at 2 mm, and the gravel discarded. Aliquots A (control) and B (treatment by irradiation) of the <63 μm fraction were obtained by hand-sieving at 63 μm, with a minimum of 100 g each, for TCLP extractions. The small amount of sand (63 μm–2 mm) remaining on the sieve was discarded. The TCLP (USEPA Method 1311) is an 18 h, pH 2.88, acetic acid extraction-test designed to assess the mobility of analytes. Although strictly designed to emulate the conditions found in municipal landfills, it is used broadly in the environmental-consulting industry to assess the potential for generation of toxic leachates. Here it is used as a relative measure of analyte mobility.

https://doi.org/10.1017/S0885715614000918 Published online by Cambridge University Press

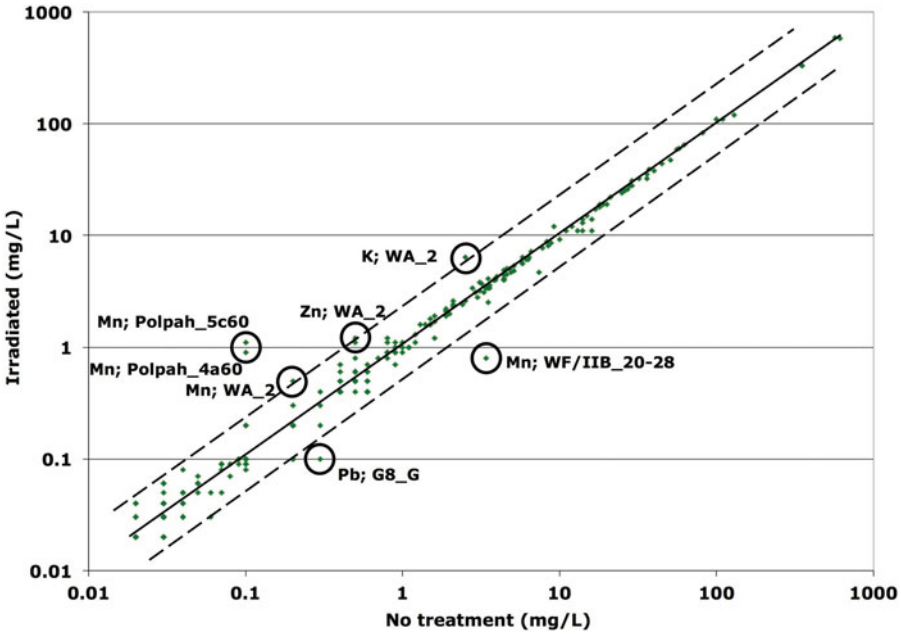

Figure 1. Concentration of all elements (Mg, Al, S, K, Ca, Cr, Mn, Fe, Ni, Cu, Zn, Zr, Cd, and Pb) from the TCLP extractions of control (no treatment) versus irradiated samples ($n = 230$ data points). A least-squares linear regression (solid line) and 95% prediction bands (dashed lines) are shown. The increased data scatter away from the regression line at concentrations <1 mg l^{-1} reflects greater analytical uncertainty associated with the ICP–AES determinations. Elements below practical quantitation limit (Table II) are not shown.

The B aliquot of the TCLP samples was subjected to 50 kGy gamma irradiation at Steritech Pty Ltd, Wetherill Park, NSW. Roughly 50 kGy was applied because it is the standard amount required by the Australian Quarantine and Inspection Service for sterilization of materials and their subsequent release from import quarantine restrictions. The samples, in 100 μm thickness polyethylene bags in a $22 \times 15 \times 10$ cm^3 cardboard box, were placed on a pallet on a conveyor belt and exposed at ambient temperature, to radiation from a ^{60}Co source for 37 h calculated at 1.35 kGy h^{-1} at the samples. This irradiation would have caused sample heating of <1 °C (Steritech P/L, personal communication, 27 March 2014).

TCLP extractions, ICP–AES analyses and associated blank, five duplicates, and six spikes forming the QA/QC program (equal to 22% of sample analyses) were undertaken at Envirolab Pty Ltd., Chatswood, NSW, which is accredited by Australia's National Association of Testing Authorities. The TCLP followed USEPA Method 1311, on 100 g of soil, owing to sample size-limitations for some of the rarer soil types. The leachates were analyzed for Mg, Al, S, K, Ca, Ti, Cr, Mn, Fe, Ni, Cu, Zn, As, Se, Zr, Cd, Sn, Sb, and Pb.

Powder X-ray diffractograms were collected from mineral samples before and after irradiation. For this analysis, 100 mg of powder was placed on a Si-crystal low-background holder for analysis. X-ray diffractograms from 5° to 90° 2θ were collected with a PANalytical X'Pert Pro MPD diffractometer, using 45 kV, 40 mA, Cu$K\alpha$ radiation, X'Celerator detector, Bragg–Brentano geometry, and a slew rate of 5°2θ per minute. Identification of minerals was undertaken with PANalytical's Highscore Plus software v2.2.4, with ICDD PDF2 and PAN-ICSD databases. Mineralogy of one sample ("Polpah_Nodules") was measured in the field in transmission geometry using a portable Olympus. Terra diffractometer using settings of 5°–55°2θ, Co$K\alpha$ radiation, peltier-cooled strip charge-coupled detector and a data collection time of 30 min (Sarrazin *et al.*, 2009). Data were examined using PANalytical's Highscore Plus software as per the laboratory instrument.

III. RESULTS AND DISCUSSION

All spike recoveries averaged 91–109% except for Zr and Sb (83%), S (114%), and Se 117%). All TCLP leachate analyses for all analytes and samples (Table II) are plotted in Figure 1 to examine for differences in leachability as a result of irradiation. A least-squares linear-regression line (slope = 0.98) reveals no effect on leachability because of irradiation. Greater scatter of data around the regression line at concentrations <1 mg l^{-1} reflect greater analytical uncertainty associated with the ICP–AES determinations.

Seven data points lie outside of the 95% prediction intervals: five analytes from three samples indicate a greater leachability and two analytes from two samples indicate a lesser leachability with irradiation. Of the seven data points, four relate to Mn, with the remainder from K, Zn, and Pb. The minerals that host these analytes are all below detection limits using X-ray diffractometry, so it is not possible to understand further why these samples behaved in this way. However, X-ray diffractometry analysis of hand-picked oxide-covered fine gravels from the "Polpah" field area near White Cliffs in the semi-arid zone of Eastern Australia revealed the presence of the hydrated manganese oxide birnessite [$K_{0.296}Mn_{0.926}O_2(H_2O)_{0.42}$] as the only Mn-bearing phase (Figure 2), and it may be that this mineral is prone to decomposition by gamma irradiation. However, the distribution of this small number of outliers to either side of the regression line suggests that there is no systematic effect of gamma irradiation on the mineral suites in these soils and as a result the remainder of the diffractograms are not presented. As the

https://doi.org/10.1017/S0885715614000918 Published online by Cambridge University Press

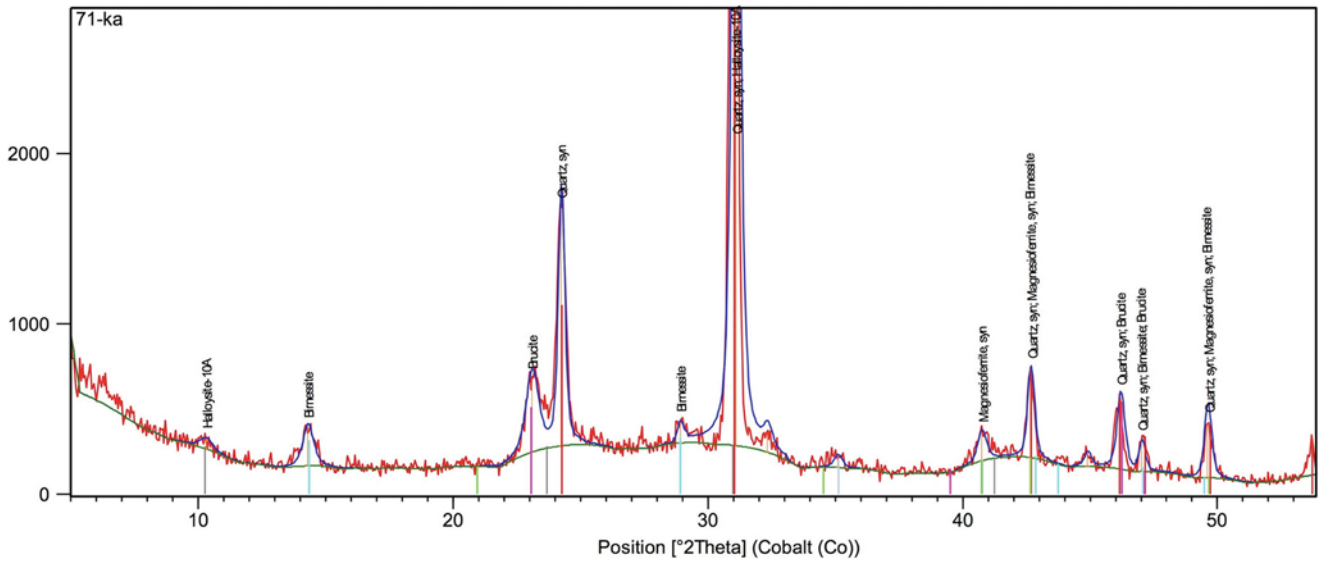

Figure 2. Diffractogram of pisolitic gravels in the Polpah area near White Cliffs, NSW, comprised of quartz, birnessite [$K_{0.296}Mn_{0.926}O_2(H_2O)_{0.42}$], brucite [$Mg(OH)_2$], and possibly halloysite [$Al_2Si_2O_5(OH)_4.2H_2O$]. The *Y*-axis is total counts.

original samples were divided into two aliquots, it is likely that what is being observed with these few samples is simply the nugget effect, whereby occasional enrichment or depletion of an element in an aliquot results from the heterogeneous distribution of compositionally unusual particles in that aliquot and not the other.

Ionizing radiation can create defects in and amorphization of clays, including kaolinite, dickite, montmorillonite, and illite, and other minerals including apatite and the zeolite family (Wang *et al.*, 2004; Allard and Calas, 2009). Radiation damage to some minerals, including some of the zeolite family, can reduce desorption characteristics dramatically (Wang *et al.*, 2004) which is of relevance to our research question. However, reports on the effects of gamma irradiation on the propensity for enhanced or inhibited leaching are contradictory. In contrast to the reduced desorption noted by Wang *et al.* (2004), enhanced leaching of Co from zeolites and a clay were reported following 7670 kGy gamma irradiation (Dávila-Rangel *et al.*, 2007) and the formation of a new potassium calcium silicate indicated extensive structural damage to the sample mineralogy, particularly to a zeolite. Zero-valent Cu immersed in water showed thin (50–100 nm) but clearly visible surface-oxidation damage following 35–74 kGy of gamma irradiation, with ~20–74 kGy of gamma irradiation causing increases in aqueous-Cu concentration in the surrounding water (Björkbacka *et al.*, 2013). The damage was reported to occur via corrosion enhanced by the radiolysis products of water, possibly enhanced by galvanic action at the Cu surface. Roughly 84 kGy of gamma irradiation reduced iron in sodium montmorillonite temporarily, with the effects disappearing after 3 weeks. The mechanism proposed was radiolysis of interlayer water followed by structural annealing or iron re-oxidation (Gournis *et al.*, 2000), but this radiolysis of water did not manifest as changes to interlayer spacings and so were not detected on X-ray diffractograms (Gournis *et al.*, 2001).

Reconciling these differences in material behavior in response to gamma irradiation is complex, depending on total radiation received, irradiation rate, the material, water content, and temperature. Further research may be required before more generalized statements regarding the effects of 50–100 kGy of gamma irradiation on natural soils can be made. However for our dry, mineral materials, it may be either that 50 kGy of gamma radiation does not affect mineral samples permanently, or if it does then the damage is small enough that no detectable changes to leachability occur, as demonstrated by our TCLP extractions. In either case, 50 kGy of gamma irradiation is sufficient to release mineral samples from Australian quarantine restrictions, allowing subsequent experimentation without detriment to the results.

IV. CONCLUSION

We conclude from the present study that it is possible to release a wide range of mineral soils and sediments from quarantine, via 50 kGy gamma irradiation, with no implications for subsequent inorganic chemical experimentation.

ACKNOWLEDGEMENT

We acknowledge the Australian Antarctic Division for financial support under AAS4029.

Allard, Th. and Calas, G. (**2009**). "Radiation effects on clay mineral properties," Appl. Clay Sci. **43**, 143–149.

Aygun, Z., Aygun, M., Karabulut, B., and Karabulut, A. (**2012**). "Investigation of non-irradiated and gamma-irradiated Trommel Sieve Waste (TSW) with EPR technique," Ann. Nucl. Energy **40**, 84–86.

Björkbacka, Å., Hosseinpour, S., Johnson, M., Leygraf, C., and Jonsson, M. (**2013**). "Radiation induced corrosion of copper for spent nuclear fuel storage," Radiat. Phys. Chem. **92**, 80–86.

Brown, K. A. (**1981**). "Biochemical activities in peat sterilized by gamma-irradiation," Soil Biol. Biochem. **13**, 469–474.

Corbett, W. J., Burson, J. H., and Young, R. A. (**1963**). "Gamma-irradiation of kaolinite," Clays Clay Mineral. **10**, 344–355.

DAFF (**2013**). Australian Government, Department of Agriculture, Fisheries and Forestry. http://www.daff.gov.au/aqis/import/general-info/qtfp/contamination-treatment-guide

https://doi.org/10.1017/S0885715614000918 Published online by Cambridge University Press

Da Silva, D. N., Guedes, K. J., Pinheiro, M. V. B., Spaeth, J. M., and Krambrock, K. (**2005**). "The microscopic structure of the oxygen–aluminium hole center in natural and neutron irradiated blue topaz," Phys. Chem. Miner. **32**, 436–441.

Dávila-Rangel, J. I. and Solache-Ríos, M. (**2008**). "Cadmium leaching from thermal treated and gamma irradiated Mexican aluminosilicates," J. Nucl. Mater. **380**, 120–125.

Dávila-Rangel, J. I., Solache-Ríos, M., and Nuñez-Monreal, J. E. (**2007**). "Radiation and thermal effects on cobalt retention by Mexican aluminosilicates," J. Nucl. Mater. **362**, 53–59.

Dias, L. N., Pinheiro, M. V. B., and Krambrock, K. (**2009**). "Radiation-induced defects in euclase: formation of O^{-} hole and Ti^{3+} electron centers," Phys. Chem. Miner. **36**, 519–525.

Eno, C. F. and Popenoe, H. (**1964**). "Gamma radiation compared with steam and methylbromide as a soil sterilizing agent," Proc. Soil Sci. Soc. Am. **28**, 533–535.

Fattahi, M., Houée-Levin, C., Ferradini, C., and Jacquier, P. (**1992**). "Hydrogen peroxide formation and decay in gamma-irradiated clay water," Int. J. Radiat. Appl. Instrum. **C40**, 167–173.

Gournis, D., Mantaka-Marketou, A. E., Karakassides, M. A., and Petridis, D. (**2000**). "Effect of γ-irradiation on clays and organoclays: a Mössbauer and XRD study," Phys. Chem. Miner. **27**, 514–521.

Gournis, D., Mantaka-Marketou, A. E., Karakassides, M. A., and Petridis, D. (**2001**). "Ionizing radiation-induced defects in smectite clays," Phys. Chem. Miner. **28**, 285–290.

Holmboe, M., Wold, S., Jonsson, M., and García-García, S. (**2009**). "Effects of γ-irradiation on the stability of colloidal Na^{+}-Montmorillonite dispersions," Appl. Clay Sci. **43**, 86–90.

Holmboe, M., Jonsson, M., and Wold, S. (**2012**). "Influence of γ-radiation on the reactivity of montmorillonite towards H_2O_2," Radiat. Phys. Chem. **81**, 190–194.

Jackson, N. E., Corey, J. C., Frederick, L. R., and Picken, J. C. Jr (**1967**). "Gamma irradiation and the microbial population of soils at two water contents," Proc. Soil Sci. Soc. Am. **31**, 491–494.

Kinchin, G. H. and Pease, R. S. (**1955**). "The displacement of atoms in solids by radiation," Rep. Prog. Phys. **18**, 1–51. http://iopscience.iop.org/0034-4885/18/1/301.

Krambrock, K., Pinheiro, M. V. B., Guedes, K. J., Medeiros, S. M., Schweizer, S., and Spaeth, J. M. (**2004**). "Correlation of irradiation-induced yellow color with the O-hole center in tourmaline," Phys. Chem. Miner. **31**, 168–175.

Martinez-Gallegos, S. and Bulbulian, S. (**2004**). "Effects of γ radiation on chromate immobilization by calcined hydrotalcites," Clays Clay Miner. **52**, 650–656.

McLaren, A. D., Luse, R. A., and Skujins, J. J. (**1962**). "Sterilization of soil by irradiation and some further observations on soil enzyme activity," Proc. Soil Sci. Soc. Am. **26**, 371–377.

Negron, A., Ramos, S., Blumenfeld, A. L., Pacheco, G., and Fripiat, J. J. (**2002**). "On the structural stability of montmorillonite submitted to heavy γ –irradiation," Clays Clay Miner. **50**, 35–37.

Northcote, K. H. (**1979**). *A Factual Key for the Recognition of Australian Soils* (Rellim Technical Publishers, Glenside, South Australia), 4th ed.

Pantelides, S. T., Lu, Z.-Y., Nicklaw, C., Bakos, T., Rashkeev, S. N., Fleetwood, D. M., and Schrimpf, R. D. (**2008**). "The E′ center and oxygen vacancies in SiO_2," J. Non-Crystal. Solids **354**, 217–223.

Plötze, M., Kahr, G., and Stengele, R. H. (**2003**). "Alteration of clay minerals – gamma-irradiation effects on physicochemical properties," Appl. Clay Sci. **23**, 195–202.

Popenoe, H. and Eno, C. F. (**1962**). "The effect of gamma radiation on the microbial population of the soils," Soil Sci. Soc. Am. J. **26**, 164–167.

Pushkareva, R., Kalinichenko, E., Lytovchenko, A., Pushkareva, A., Kadochnikova, V., and Plastynina, M. (**2002**). "Irradiation effect on physicochemical properties of clay minerals," Appl. Clay Sci. **21**, 117–123.

Sarrazin, P., Chiari, G., and Gailhanou, M. (**2009**). "A portable non-invasive XRD-XRF instrument for the study of art objects," pp. 175–186. JCPDS-International Centre for Diffraction Data 2009 ISSN 1097-0002. http://www.icdd.com/resources/axa/vol52/v52_23.pdf

Stark, S. C., Snape, I., Graham, N., Brennan, J., and Gore, D. B. (**2008**). "Assessment of metal contamination using X-ray fluorescence spectrometry and the toxicity characteristic leaching procedure (TCLP) during remediation of a waste disposal site in Antarctica," J. Environ. Monitor. **10**, 60–70.

USEPA Method 1311 – Toxicity Characteristic Leaching Procedure. http://www.epa.gov/osw/hazard/testmethods/sw846/pdfs/1311.pdf

USEPA Method 1312 – Synthetic Precipitation Leaching Procedure, http://www.epa.gov/osw/hazard/testmethods/sw846/pdfs/1312.pdf

Wang, L. M., Chen, J., and Ewing, R. C. (**2004**). "Radiation and thermal effects on porous and layer structured materials as getters of radionuclides," Current Opin. Solid State Mater. Sci. **8**, 405–418.

https://doi.org/10.1017/S0885715614000918 Published online by Cambridge University Press